 MCB, vol.4, no.4, pp.177-188, 2007

Focal Adhesion Kinase Signaling Controls Cyclic Tensile Strain Enhanced Collagen I-Induced Osteogenic Differentiation of Human Mesenchymal Stem Cells

Donald F. Ward Jr.[*], William A. Williams[*], Nicole E. Schapiro[*], Samuel R. Christy[*] Genevieve L. Weber[*], Megan Salt, Robert F. Klees[*], Adele Boskey[†], and George E. Plopper[*,‡]

Abstract: Focal adhesion kinase (FAK) is a key integrator of integrin-mediated signals from the extracellular matrix to the cytoskeleton and downstream signaling molecules. FAK is activated by phosphorylation at specific tyrosine residues, which then stimulate downstream signaling including the ERK1/2 pathway, leading to a variety of cellular responses. In this study, we examined the effects of FAK point mutations at tyrosine residues (Y397, Y925, Y861, and Y576/7) on osteogenic differentiation of human mesenchymal stem cells exposed to collagen I and cyclic tensile strain. Our results demonstrate that FAK signaling emanating from Y397, Y925, and to a lesser extent Y576/7, but not from Y861, controls osteogenic differentiation through an ERK1/2 pathway, as measured by expression levels of key osteogenesis marker genes and subsequent matrix mineralization. These data indicate that FAK is a critical decision maker in extracellular matrix/strain-enhanced osteogenic differentiation.

Keyword: Tensile strain, Osteogenesis, hMSC, FAK, Point Mutagenesis, Collagen-I ECM, Gene Expression, Mineralization

[*] Department of Biology, Rensselaer Polytechnic Institute, Troy, NY 12180-3596, USA

[†] Hospital for Special Surgery, New York City, NY 10021, USA

[‡] Corresponding author. Center for Biotechnology and Interdisciplinary Studies, BCHM-2, Rensselaer Polytechnic Institute, 110 8^{th} St, Troy, NY 12180, Phone: (518) 276-6332, Fax: (518) 276-2851, Email: ploppg@rpi.edu

1 Introduction

Integrin-mediated binding to the extracellular matrix (ECM) stimulates intracellular signaling pathways that control cell proliferation, migration, and differentiation. One of the first downstream regulators of integrin signaling is the protein tyrosine kinase known as focal adhesion kinase (FAK). While it is well known that FAK controls the growth and migration of multiple cell types, its role in controlling cellular differentiation is not as well known. We and others have demonstrated a role for FAK in the differentiation of mesenchymal cells, including human mesenchymal stem cells (hMSC) and their more differentiated progeny, chrondrocytes and preosteoblasts (1-4). The molecular mechanisms governing FAK-mediated phenotype commitment of stem cells are almost entirely unknown.

FAK exists in multiple activation states, based on the phosphorylation of key tyrosine residues (e.g., Y397, Y576/7, Y861, and Y925) within the protein (5-9). Phosphorylation of these residues triggers activation of FAK kinase activity (at Y576/7) and promotes the binding of additional signaling proteins (at Y397, Y925, and Y861) that propagate signals further downstream (10). One of these additional proteins is the tyrosine kinase Src (11), which binds phosphorylated Y397 via its SH2 domain and acts in concert with FAK to activate both the PI3K-Akt pathway and the Grb2-Sos-Ras-ERK pathway (7, 12). In both hMSCs and osteoblasts, activation of ERK1/2 promotes osteogenic differentiation by activating and/or inducing expression of key osteogenic transcription factors (13-15). Thus, FAK signaling through ERK1/2 may represent one of the earliest decision

Table 1: qRT-PCR primer pairs for osteogenic genes (osterix, osteocalcin, and bone sialoprotein 2) and GAPDH, as well as, the RT-PCR primer pair for c-Myc-PTK2. Accession number, sequence composition, and fragment size are listed for the genes.

Gene Name	Primer Sequences	Product Size (bp)
Osterix NM_152860	Forward 5' - GCCAGAAGCTGTGAAACCTC - 3' Reverse 5' - GCTGCAAGCTCTCCATAACC - 3'	457
Osteocalcin NM_199173	Forward 5' - GACTGTGACGAGTTGGCTGA - 3' Reverse 5' - CTGGAGAGGAGCAGAACTGG - 3'	400
Bone Sialoprotein 2 NM_004967	Forward 5' - CTGCTTCCTCACTCCAGGAC - 3' Reverse 5' - GATTGCTTCCTCTGGCAGTC -3'	401
GAPDH (Glyceraldehyde-3-phosphate dehydrogenase) NM_002046	Forward 5' - CGACCACTTTGTCAAGCTCA - 3' Reverse 5' - AGGGGTCTACATGGCAACTG - 3'	1000
C-myc-PTK2 (C-myc epitope on N-terminus of FAK)	Forward 5' -AGAAGCTGATCTCCGAGGAGGACC - 3' Reverse 5' -CAGGTGACTGAGGCGAAATCCATA - 3'	296

making events controlling hMSC commitment to the osteogenic phenotype.

In hMSCs cultured *in vitro*, the ERK pathway is sensitive to mechanical strain (14) and integrin binding to ECM (13). Mechanical strain alters gene expression via ERK through integrin-ECM binding (16-19). We have recently demonstrated that application of cyclic tensile strain promotes osteogenic differentiation of these cells, as assessed by osteogenic gene expression and matrix ossification (mineral:matrix ratio), through an ERK-dependent pathway (20). In this study, we tested the hypothesis that disrupting FAK signaling emanating from key tyrosine residues, by overexpressing point mutants where the tyrosines have been replaced with phenylalanines, decreases mechanical strain-enhanced, collagen-I (COL-I) induced osteogenic differentiation of hMSCs. Our results demonstrate that a subset of these tyrosines is responsible for stimulating ERK1/2 and osteogenic differentiation under these conditions.

2 Materials and Methods

Tissue culture media (DMEM) and penicillin G-streptomycin sulfate (GPS) were purchased from Mediatech (Cellgro, VA). Fetal bovine serum (FBS) was purchased from Gemini Bio-Products (Woodland, CA). Trypsin-EDTA was obtained from Sigma Chemical Co. (St. Louis, MO). COL-I coated and uncoated silicone rubber BioFlex™ 6-well plates were purchased from FlexCell International Corporation (Hillsborough, NC). Rabbit polyclonal IgG antibodies against anti-phosphotyrosine FAK 861 (catalog # 07-832) and 576/7 (catalog # 07-157), and anti-ERK1/2 (catalog # AB3053) were obtained from Chemicon International (Temecula, CA). Mouse polyclonal IgG antibody against anti-phosphotyrosine FAK 397 (catalog # MAB1144) was obtained from Chemicon International (Temecula, CA). Rabbit monoclonal IgG antibody against anti-FAK (catalog # 04-591) was obtained from Chemicon International (Temecula, CA). Rabbit polyclonal IgG phosphospecific antibody against anti-ERK 1/2 ($pTpY^{185/187}$) (catalog # 44-680) was from Biosource International (Camarillo, CA). Goat polyclonal IgG antibody against anti-phosphotyrosine FAK 925 (catalog # sc-11766) was obtained from Santa Cruz Biotechnology (Santa Cruz, CA). Horseradish peroxidase (HRP)-conjugated secondary antibodies were obtained from Jackson Immuno Research (West Grove, PA). Quantitative real-time reverse transcriptase-

polymerase chain reaction (qRT-PCR) primers listed in Table 1 were purchased from IDT Technologies (Coralville, Iowa). The protein assay kit was purchased from Pierce (Rockford, IL). Unless otherwise specified, the other standard reagents were obtained from Fisher Scientific (Fair Lawn, NJ).

2.1 Cell culture

Cryopreserved hMSC were purchased from Cambrex Inc. (Walkersville, MD) and were grown according to the manufacturer's instructions. Briefly, cells were plated at 5 x 10^3 cells/cm^2 in a T75 flask (75 cm^2) for continuous passaging in DMEM medium supplemented with 10% FBS, penicillin G [10,000 units/mL] and streptomycin sulfate [10,000 μg/mL]. Medium was changed twice weekly and cells were detached by trypsin-EDTA and passaged into fresh culture flasks at a ratio of 1:3 upon reaching confluence. Cultures were incubated at 37°C in a humidified atmosphere containing 95% air and 5% CO_2.

2.2 Retroviral Infection of hMSC

hMSC were infected with retroviruses engineered to overexpress myc-tagged point mutants of FAK (tyrosine residues 397, 576/577, 861, or 925 were replaced with a phenylalanine), myc-tagged wild-type FAK, or myc-tagged blank vectors (NEO) as described previously (21). Briefly, retroviruses for transduction of hMSCs were produced using the MSCV retroviral expression system (catalog # 634401) from BD Biosciences Clontech (Palo Alto, CA). The genes coding for c-myc epiotope-tagged FAK and FAK Y397F, Y925F, Y576/7F, or Y861 were PCR-amplified from the pRC/CMV-c-myc-FAK expression plasmids and ligated into the pMSCVneo expression vector as restriction fragments at the *Hpa*I-to-*Bgl*II site. The mouse fibroblast retroviral packaging cell line, PT67, was transfected with the pMSCVneo/c-myc-FAK plasmids using the TransIT-3T3 transfection kit purchased from Mirus Corp. (Madison, WI). Stem cells were infected with retrovirus by duplicate 24 hour exposures to viral supernatant (from clonal, G418-resistant, transfected PT67 cell lines) containing polybrene (8 μg/mL) with an intermediate 24 hour exposure to virus-free hMSC medium. Polyclonal populations of G418-resistant hMSC ($\sim$760 μg/mL active G418 in hMSC medium) were isolated after retroviral infection. Subsequently, these cells and cells from the same lineage, but not exposed to viral supernatant (i.e., the control group) were plated as described above. G418 antibiotic pressure was maintained on the infected cell lines throughout in the culture media.

2.3 Mechanical strain application

For in vitro osteogenic assays, hMSCs were passaged three times before they were plated at densities of 12,500 cells/cm^2 in 0.3 mL/cm^2 of medium on 6-well flexible silicone rubber BioFlex™ plates (57.75 cm^2 total area). The cells were cultured for 48 hours to allow them to proliferate, grow, attach to the COL-I ECM, and spread out and reach 80 to 90% confluency, at which time the culture medium was replaced. For the short term signaling pathway analyses (Figures 2 and 3), the cells were then serum deprived with only 1% FBS for 24 hours to reduce FAK and ERK activation to basal levels. The long term osteogenic differentiation and gene expression studies were provided with new 10% FBS culture media as in normal media changes. In each experiment, control and strained cells were processed in parallel.

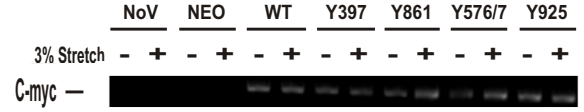

Figure 1: Expression of exogenous c-myc-FAK in virus-infected hMSC. RT-PCR amplification of the c-myc-FAK transcript was observed in hMSCs infected with c-myc-FAK (wild type (WT);lanes 5 and 6), c-myc-FAK Y397F (lanes 7 and 8), c-myc-FAK Y861F (lanes 9 and 10), c-myc-FAK Y576/7F (lanes 11 and 12), and c-myc-FAK Y925F viruses (lanes 13 and 14) and not in uninfected, control hMSCs (WT;lanes 1 and 2) or in hMSCs infected with the NEO blank vector (lanes 3 and 4).

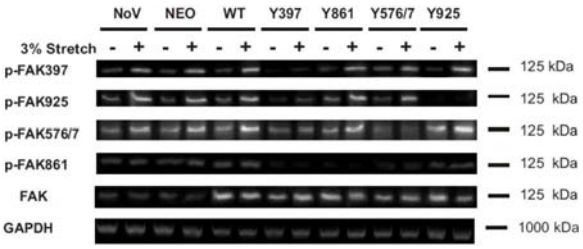

Figure 2: Mechanical strain increases FAK activation in hMSC and dominant negative point mutations of FAK mitigate this effect. The same hMSC cell types as in Figure 1 were plated on COL-I coated silicone rubber membranes and were either strained, with a 3% cell size increase 0.5 Hz. cyclic tensile strain, or without strain for 30 minutes then probed by immunoblot for pY397 FAK (top row), pY925 FAK (second row), pY576/7 FAK (third row), pY861 FAK (fourth row), total FAK (fifth row), or GAPDH (bottom row). GAPDH was used as a loading control.

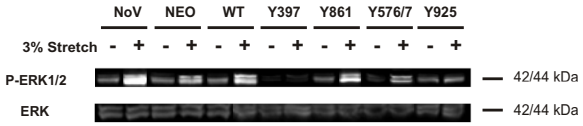

Figure 3: Mechanical strain increases ERK activation in hMSC and dominant negative point mutations of FAK decrease this effect. The same hMSC cell types as in Figure 1 were plated, strained, and processed as in Figure 2. Immunoblotting was for pTpY185/187 ERK 1/2 (top row) and total ERK (bottom row).

Estimates of the physiological range of mechanical forces on bone (and especially fracture callus, where hMSC are most concentrated) vary widely, and 0.1-18% tensile strain has been used for in vitro studies of osteoblast differentiation (21, 22). This study used 3% cell size increase, closer to the most common estimates of 1-6%. The strain was applied using an FX-4000T™ Flexercell® Tension Plus™ unit (Flexcell International, Hillsborough, North Carolina). A sinusoidal curve waveform strain application was applied at a frequency of 0.5 Hz. The stain was applied continuously for the short duration signaling pathway studies (Figures 2 and 3) or for 2 hours per day with eight 15 minute strain periods for the longer strain regimens. Additionally, the longer term experiments involved a strain regimen of only 2 hours per day in 15 minutes blocks. Following the first seven 15 minute stretching periods were two hour breaks and an eight hour break followed the eighth 15 minute stretch. These breaks allowed the cells time to interpret and process the stimulus without the cyclic tensile strain stress and represent the alternating increased and reduced strains that bones experience *in vivo*. ™™edium was still changed twice weekly and the cultures were also incubated at 37°C in a humidified atmosphere containing 95% air and 5% CO_2. At various time points, cultures were assayed as described below.

2.4 Mineralized bone: Fourier transform infrared (FTIR) analysis

FTIR analysis of the insoluble matrix provided a quantitative mineralization measure of the calcium phosphate cross-linked hydroxyapatite crystal formation of the secreted COL-I ECM protein, the ultimate endpoint to bone formation, expressed as the mineral:matrix ratio. The presence of apatite in cell matrix was detected by FTIR of ground powders. Cell layers, collected in 50 mM ammonium bicarbonate (pH 8.0) after 28 days culture in the presence or absence of tensile strain, were lyophilized and analyzed as potassium bromide (KBr) pellets on a Bio-Rad FTS 40-A spectrometer (Bio-Rad, Cambridge, MA). The data was collected under nitrogen purge, and the spectral baseline corrected and analyzed using GRAMS/386 software (Galactic Industries, Salem, NH) as previously described (22). The mineral content was calculated based on the spectrally derived mineral-to-matrix ratio, that is, the ratio of the spectral area of the phosphate absorbance peak (900-1200 cm^{-1}) to the spectral area of the protein amide I peak (1585-1720 cm^{-1}). The experimental outcomes were compared to the relevant control using the areas of these two peaks – an experiment with a larger phosphate peak and a smaller amide peak than its control has a higher mineral-to-matrix ratio.

2.5 Immunoblot analysis

Whole cell extracts were prepared by harvesting cells with ice-cold radio immunoprecipitation assay buffer (150 mM NaCl, 50 mM Tris, 1% Triton-X, 0.3 mM Sodium vanadate, 1% Deoxycholic acid, 0.2% SDS, pH 7.4) supplemented with protease inhibitor cocktail (Sigma). The lysate was centrifuged at 2,500 g for 10 seconds before a fraction of the supernatant was sequestered for a protein assay. Subsequently, protein concentration of the supernatant was determined by the BCA method (Pierce, Rockland IL). Equal amounts of protein for each sample, resuspended in Laemmli sample buffer, were denatured at 100?C for 5 minutes, resolved by 8% SDS-PAGE, and electrophoretically transblotted to Trans-Blot® nitrocellulose membranes (0.2 μm) (Bio-Rad, Hercules, CA). The membranes were incubated with blocking solution (5% nonfat dried milk in 1 *times* PBS + 0.2% Tween-20 (PBST)) for 1 hour, then probed with various primary antibodies (1:500 in PBST) overnight at 4°C. After three washes with PBST, membranes were incubated with HRP-conjugated secondary IgG (1:25,000) for 1 hour, followed by another three washes with PBST. Immunoreactive bands were visualized using the SuperSignal® Chemiluminescent reagent (Pierce) and captured using a ChemiImager 4400 Gel imaging system (Alpha Innotech, San Leandro, CA).

2.6 Reverse transcriptase-polymerase chain reaction (RT-PCR) and quantitative real-time RT-PCR (qRT-PCR) Analysis

RNA was isolated from hMSC at 1 week by pooling together the cells scraped from 2 wells of the BioFlex™ 6-well plates. Total RNA was isolated using the RNeasy mini kit (Qiagen, Valencia, CA). qRT-PCR was performed with the QuantiTect® SYBR Green RT-PCR Kit with HotStar Taq DNA Polymerase (Qiagen) and a Roche LightCycler® 480 Real-Time PCR System (Roche, Pleasonton, CA). Melting curve analysis confirmed that the targeted mRNA was being amplified specifically. RT-PCR was performed with the OneStep RT-PCR Kit (Qiagen) and a 96 well thermal cycler (MJ Research, Waltham, MA). The primers used are listed in Table 1 and were designed using OligoPerfect™ (Invitrogen, Carlsbad, CA) and purchased through IDT Technologies. Three-hundred nanograms of template RNA was used per reaction. Real-time qRT-PCR was performed according to the following protocol defined by the manufacturer: RT 20min at 50°C 20°C/s ramp, PCR activation 15min at 95°C 20°C/s ramp, 40 cycles of [Denaturation 15s at 94°C 20/s ramp, Annealing 30s at 56°C 20°C/s ramp, Extension 30s 72°C 2°C/s ramp]. All samples were normalized to total RNA content and to the performance of the housekeeping gene, GAPDH. The RT-PCR was performed as follows: The reverse transcription step ran for 30 minutes at 50°C, followed by PCR activation for 15 minutes at 95°C. Thirty amplification cycles were run, consisting of one minute denaturation at 94°C, one minute of annealing at 58°C, and one minute of extension at 72°C. Final extension was allowed to run 10 minutes at 72°C. RT-PCR reaction products were separated by gel electrophoresis using a 1.2% agarose gel. Bands were visualized by UV illumination of ethidium-bromide-stained gels and captured using a ChemiImager 4400 Gel imaging system (Alpha Innotech, San Leandro, CA).

2.7 Statistical analysis

All experiments were repeated at least three times and the representative data were presented as mean $\pm$ standard deviation. Statistical analyses were preformed using Student's unpaired t test, and a p value less than 0.05 was considered significant.

3 Results

3.1 Retrovirally infected dominant negative hMSC FAK mutants express c-myc-tag

We used RT-PCR amplification of the c-myc-FAK mRNA to show that the c-myc-FAK gene is expressed by hMSC after retroviral infection (Figure 1). Only a c-myc-FAK region of the exogenous gene was amplified, because the forward primer used binds to the 5' region of the c-myc gene, and the reverse primer binds $\sim$300 bp downstream in

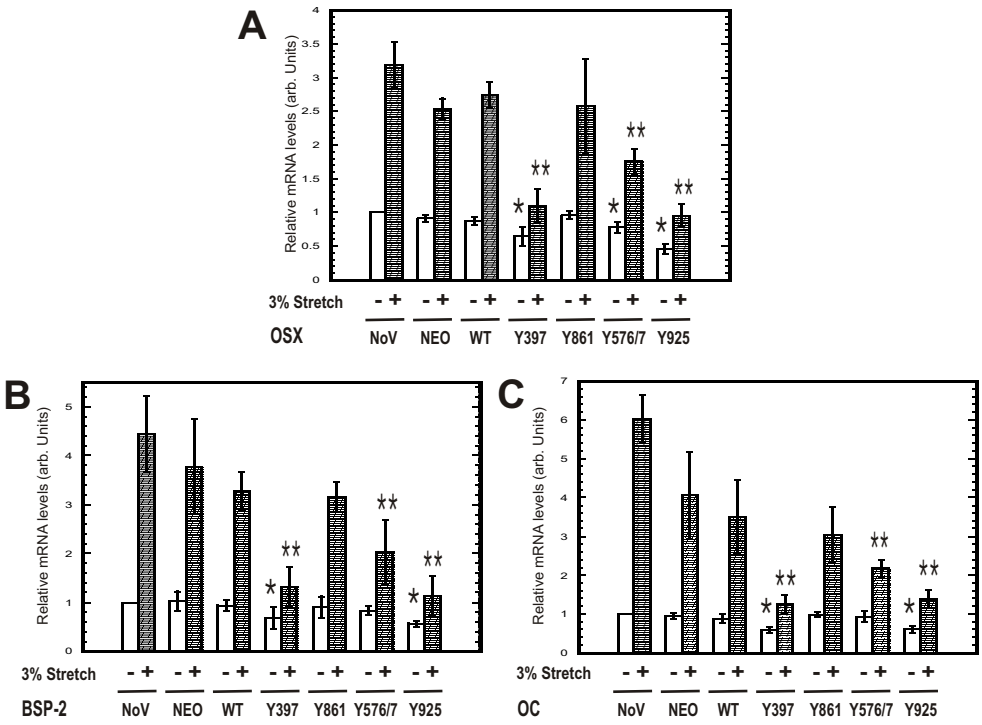

Figure 4: Mechanical strain increases expression of osteogenic genes in hMSC and dominant negative point mutations of FAK inhibit this effect. The same hMSC cell types as in Figure 1 were plated as in Figure 2 and either strained as described in the materials and methods section above or without strain for 7 days. Real-time quantitative RT-PCR (qRT-PCR) was performed to amplify the mRNA of key osteogenic marker genes using the primers listed in Table 1. GAPDH was amplified as a loading control. Panel A: qRT-PCR of the osteogenic transcription factor osterix mRNA. Panel B: qRT-PCR of the osteogenic bone protein bone sialoprotein 2 mRNA. Panel C: qRT-PCR of the osteogenic bone protein osteocalcin mRNA. Asterisks and double asterisks indicate significant ($p<0.05$) increases as compared to the parallel uninfected (NoV) control samples using Student's unpaired t test.

the region of the gene coding for FAK. Therefore, endogenous myc and FAK genes were not transcribed (23). This 300 bp RT-PCR product was produced from total RNA of c-myc-FAK infected hMSCs, containing the wild-type or the mutant c-myc-FAK genes (Figure 1; lanes 5 through 14), but not from total RNA of hMSCs without any infection (Figure 1; lanes 1 and 2), or containing only the blank NEO vector (Figure 1; lanes 3 and 4).

3.2 Cyclic tensile strain causes FAK phosphorylation in hMSC plated on COL-I, and FAK signaling is disrupted by myc-tagged point mutants of FAK

We used immunoblotting with phospho-specific antibodies for FAK residues Y397, Y576/7, Y861, and Y925 as well as an antibody against an unmodified epitope on FAK, to show that retroviral infection with c-myc-tagged FAK constructs increased the total amount of FAK in hMSC but disrupted FAK phosphorylation at these amino acids (Figure 2). Levels of total FAK were elevated in all c-myc-FAK infected hMSCs (lanes 5-14), as compared to hMSCs infected with the blank vector (NEO-lanes 3 and 4) and without any infection (NoV-lanes 1 and 2). Application of a cyclic tensile strain to cells not expressing FAK mutants increased levels of phosphorylated FAK at Y397, Y925, and Y576/7, but not at Y861. Infection with Tyr→Phe dominant negative mutants targeting theses residues in FAK decreased phosphorylation levels of all FAK at these residues, in both the strained and unstrained conditions. The

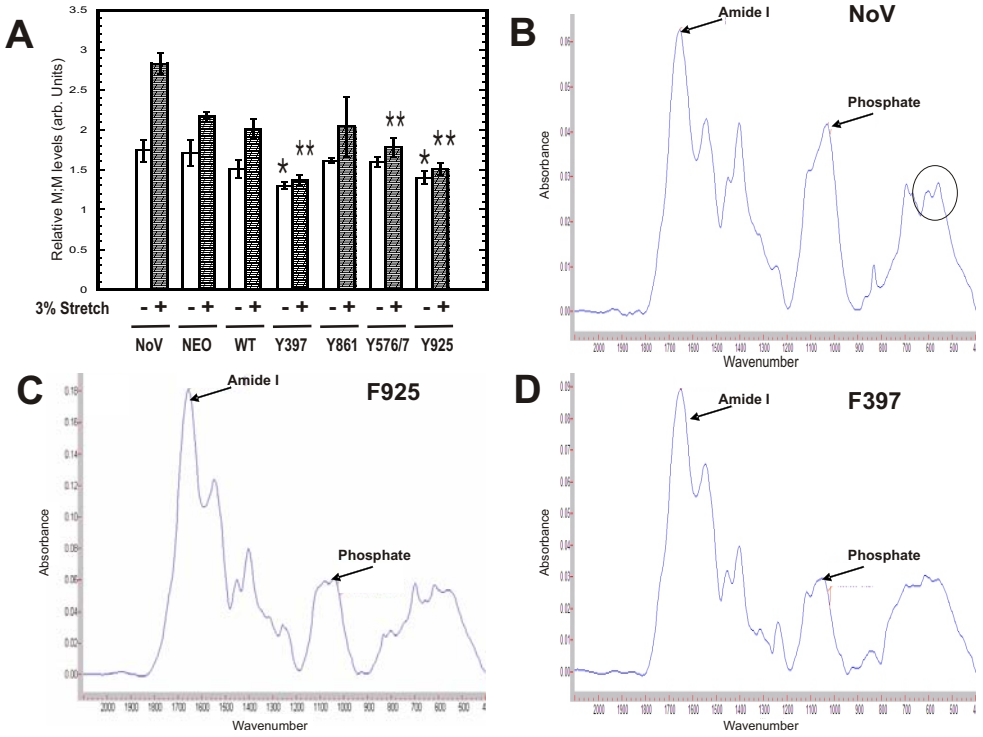

Figure 5: Mechanical strain increases matrix mineralization and dominant negative point mutations of FAK mitigate this effect. The same hMSC cell typesas in Figure 1 were plated as in Figure 2 and either strained as described in the materials and methods section above or without strain for 28 days. Panel A: FTIR mineral:matrix ratio analysis comparing the relative spectral sizes of the Amide I and Phosphate peaks. Asterisks and double asterisks indicate significant ($p<0.05$) increases as compared to the parallel uninfected (NoV) control samples using Student's unpaired t test. Panels B-D: Representative FTIR spectra for uninfected, Y925F, and Y397F hMSCs with strain, respectively. Note the large Phosphate peak relative to the Amide I peak in the uninfected hMSCs as compared to that of the mutant cells. Circle represents the nu4 region (500-650 cm-1) indicating the quality of the hydroxyapatite crystals. The peak in this area indicates the level of crystallinity, whereas a broad spectral curve without a peak indicates the hydroxyapatite is poorly crystalline.

Y397 dominant negative mutation (lanes 7 and 8), and to a lesser extent, the Y576/7 dominant negative mutation (lanes 11 and 12), decreased phosphorylation levels at all the residues measured.

3.3 Dominant negative FAK mutations mitigate cyclic tensile strain-induced increases in ERK1/2 phosphorylation in hMSC plated on COL-I

Uninfected hMSCs, or those infected with the blank NEO vector or wild-type (WT) FAK, showed considerable increases in the phosphorylated levels of both pERK1 and pERK2 in response to strain (Figure 3). However, dominant negative mutations at Y397 and Y925 largely mitigated this effect (lanes 1 through 6 compared to lanes 7 and 8 and lanes 13 and 14). A dominant negative mutation at Y576/577 decreased the pERK 1 and pERK 2 levels, but to a lesser extent than that observed with the Y397 and Y925 mutants (lanes 1 through 6 compared to lanes 11 and 12). A dominant negative mutation at Y861 had little effect on the pERK 1 and 2 levels (lanes 1 through 6 compared to lanes 9 and 10).

3.4 Dominant negative FAK mutations decrease cyclic tensile strain-induced increases in osteogenic gene expression in hMSC plated on COL-I

Uninfected hMSCs and those infected with the blank NEO vector or WT FAK, showed significant increases in the expression levels of key osteogenic marker genes (osteogenic transcription factor osterix and osteogenic bone proteins osteocalcin and bone sialoprotein 2) in response to cyclic tensile strain (Figure 4). However, dominant negative mutations at Y397 and Y925 significantly reduced this effect (bars 1-6 compared to bars 7-8 and 13-14). The dominant negative mutation at Y576/577 significantly decreased the expression levels for all the osteogenic marker genes in the strained conditions, but only osterix was reduced in non-strained cells; Y397 and Y925 mutants reduced this gene expression further (bars 1-6 compared to bars 11-12). The dominant negative mutation at Y861 yielded no significant change in osteogenic gene expression in either strained or unstrained cells (bars 1-6, 9 and 10). The primers used are listed in Table 1 and GAPDH was amplified as a loading control.

3.5 Dominant negative FAK mutations inhibit cyclic tensile strain-induced increases in matrix mineralization in hMSC plated on COL-I

Uninfected hMSCs and those infected with the blank NEO vector or WT FAK, showed significant increases in matrix mineralization when exposed to strain (Figure 5). However, dominant negative mutations at Y397 and Y925 significantly inhibited this effect (bars 1-6 compared to 7-8 and 13-14). The dominant negative mutation at Y576/577 significantly decreased the matrix mineralization in the strained conditions, but to a lesser extent than that observed with the Y397 and Y925 mutants, and had no effect in unstrained cells (bars 1-6 compared to 11-12). The dominant negative mutation at Y861 had no significant effects on mineralization under any condition (bars 1-6 compared to 9-10). Figure 5 panels B-D show representative FTIR spectra for uninfected hMSCs, cells expressing the Y925 mutant, and cells expressing the Y397 mutant and exposed to strain, respectively. Note the large phosphate peak relative to the Amide I peak in the spectrum for the uninfected hMSCs (Panel B), as compared to that of the cells expressing FAK mutants (Panels C and D).

The circle in Figure 5, panel B, represents the nu4 region (500-650 cm-1), which indicates the quality of the hydroxyapatite crystals. A sharp, defined peak in this region indicates a relatively high level of crystallinity in the sample, whereas a broad spectral curve, without a peak, indicates the hydroxyapatite is poorly crystalline (24). Note the defined peak in the spectrum for the uninfected hMSCs (Panel B), as compared to that of cells expressing FAK mutants (Panels C and D).

4 Discussion

While the importance of mechanical forces in bone formation and maintenance are well established (25-31), the molecular mechanisms controlling osteogenesis in response to mechanical strain are largely unknown. Yet osteoblasts and their precursors, hMSC, are clearly responsive to mechanical strain. For example, application of biaxial strain to a flexible, two-dimensional substrate enhances the effect of osteogenic differentiation of these cells when they are cultured in media containing soluble osteogenic stimulants (dexamethazone, beta-glycerol phosphate) (14). In a three dimensional matrix composed of collagen I and fibrin, application of cyclic tensile strain to hMSC induces transient expression of two markers of vascular smooth muscle (alpha-actin and SM22) (32, 33). Similar effects have been observed for chondrogenic differentiation of these cells as well (34, 35).

Bones experience a variety of mechanical forces, such that it is nearly impossible to model the complete strain profile for any given bone with an in vitro cell culture system. Accordingly, in vitro tensile strain regimens for primary osteoblasts or osteoblast-like cell lines vary greatly, from 0.1% to 18% over a duration of 15 minutes to 21 days (21, 22, 36). To best represent the intermittent daily mechanical forces exerted on bone, all of our experiments used a cyclic tensile strain fre-

quency of 0.5 Hz with a sinusoidal curve waveform, allowing steady loading and unloading. Additionally, the longer term experiments used a strain regimen of only 2 hours per day in 15 minutes blocks. Following the first seven 15 minute stretching periods were two hour breaks and following the eighth 15 minute stretch was an eight hour break. These breaks allowed the cells time to interpret and process the stimulus without the cyclic tensile strain stress and represent the alternating increased and reduced strains that bones experience *in vivo*.

Our work demonstrates that a 3% cell size increase biaxial cyclic tensile strain applied for only two hours a day to two dimensional cultures of hMSC plated on collagen I is sufficient to induce osteogenic differentiation in the absence of any other stimulus (20). Indeed, differentiation of these cells can be controlled by simply varying the composition or stiffness of the substrate supporting them (37, 38). Collectively, these observations suggest that variations in environmental factors (e.g., soluble stimulants, 2D vs 3D substrates, composition/stiffness of supporting matrices) may help fine tune the response of these cells to tensile strain and yield different differentiated phenotypes.

Because they form structural links between the extracellular environment and the cytoskeleton, the integrins and their associated cytosolic proteins are attractive candidates for translating extracellular cues into specific cellular responses. A considerable body of work has clearly established that integrin-associated signaling pathways are capable of transducing information about the spatial organization, composition, and molecular constituents of the ECM (reviewed in 25). FAK lies at the center of the signal transduction machinery organized around integrin-cytoskeleton scaffolds, and is itself a multifunctional and highly discriminatory signaling protein. In addition to its role in controlling cell growth and migration on ECM (7) and through cell monolayers (39), FAK is also sensitive to mechanical strain (21, 40, 41) and contributes to cellular differentiation in a number of cell types (42-44). We reported that suppression of FAK with siRNA disrupts collagen I- and laminin 5-induced differentiation of hMSC in static cultures, suggesting FAK is sensitive to ECM composition in these cells (1, 3). FAK is also reported to control survival in fully differentiated osteoblasts, implying it maintains an important regulatory role in both hMSC and their differentiated progeny. In mice engineered for targeted deletion of the FAK gene in osteoblasts, the absence of FAK is compensated for by its closely related kinase, pyk2 (45).

Due to its high number of phosphorylation sites (5), FAK is able to regulate a large number of complex downstream signaling events. Ultimately, each one of these events can be traced back to a specific phosphorylation site on FAK. Thus, as a first step towards uncovering the signaling machinery linking FAK to hMSC differentiation, we elected to use the strategy employed for mapping cellular migration signaling to specific FAK residues: Mapping FAK phosphorylation using phosphospecific antibodies, then overexpressing dominant negative point mutants at these residues. Cyclic tensile strain resulted in increased levels of FAK phosphorylation in uninfected hMSCs, as well as those infected with the blank NEO vector or WT FAK, at Y397, Y925, and Y576/7, but not at Y861. This indicates that our stimulus does not activate the signaling pathways emanating from the Y861 residue.

Interestingly, increasing the expression levels of WT FAK via infection with the WT FAK vector induced only a slight increase of phosphorylation at Y576/7 but otherwise had no impact on FAK phoshorylation levels. This suggests that the activation of FAK, rather than the total amount of the FAK protein, is the limiting factor in the FAK signaling response to strain in these cells.

While each of the point mutations decreased FAK phosphorylation at their targeted residues, the Y397 point mutation resulted in considerable decreases in FAK phosphorylation at all the residues, and the Y576/7 point mutation yielded moderate decreases in FAK phosphorylation at other residues. Because Y397 phosphorylation is required for subsequent phosphorylation of the other residues, it is not surprising that the Y397 mutant impacts phosphorylation at these sites.

This fact raises one ambiguity, however: is the reduced osteogenic differentiation associated with the Y397F mutant due to specific signaling associated with this residue, or due to the resulting reduction in phosphorylation of Y576/7 and Y925 in these cells? Because the Y576/7F and Y925F mutants induced reductions in FAK phosphorylation or osteogenic gene expression that were essentially the same as that induced by the Y397F mutant, we believe that these results implicate Y576/7 and Y925 as the primary sources of osteogenic signaling in hMSC.

Regardless of which of these residues are primarily responsible for osteogenic signaling, our data strongly suggest that ERK 1/2 is the downstream target of FAK in this pathway. In other cell types, ERK activation is linked to all three of the phosphorylation sites we have identified as pro-osteogenic in hMSC, through slightly different pathways (7). In addition, ERK translocates to the nucleus in response to tensile strain in vivo (46) and mediates osteogenic differentiation of hMSC in vitro (20). In the nucleus, ERK1/2 phopshorylates and activates two key osteogenic transcription factors (15, 47).

The ultimate product of this osteogenic signaling is deposition of calcium phosphate crystals in the extracellular matrix, aka matrix mineralization. Matrix mineralization is the hallmark indicator of osteogenesis, both *in vivo* and *in vitro* (48, 49). Currently, the most sensitive and accurate method for measuring matrix mineralization levels is Fourier transform infrared (FTIR) analysis. This expresses the mineral content as a spectrally derived mineral-to-matrix ratio (24, 50) calculated by dividing the spectral area of the phosphate absorbance peak (900-1200 cm^{-1}) to the spectral area of the protein amide I absorbance peak (1585-1720 cm^{-1}). The FTIR spectrum can also indicate the quality of the hydroxyapatite crystallinity. Our Y397 and Y925 point mutants induced significantly decreased matrix mineralization levels, in both the strained and unstrained conditions, as compared to the no virus, NEO, and wild type control conditions. The Y576/7 point mutant also induced a significant, though slightly smaller, decrease in matrix mineralization in the strained cells, and had no effect in the unstrained cells. That the Y576/7 point mutation was preferentially effective in strained cells indicates that the signaling emanating from these tyrosine residues, which are located in FAK's kinase domain, may be especially responsive to a cyclic tensile strain/COL-I stimulus.

During periods of rapid bone formation, the first hydroxyapatite precipitate is poorly crystalline along a disordered collagen network. This is later resorbed and replaced with more organized collagen fibers and a higher quality crystalline hydroxyapatite, leading to stronger bone tissue. Comparing the FTIR spectra allows one to measure relative levels of hydroxyapatite crystallinity. The sharper peak in the nu4 region (500-650 cm-1) of the no virus spectrum, as compared to that of the Y925F and Y397F spectra, shows that both of these point mutations led to decreased crystalline size and structure quality, indicative of a weaker bone phenotype.

Collectively, our results suggest that FAK is a critical decision making protein during osteogenic differentiation induced by cyclic tensile strain applied to a COL-I substrate. Specifically, pro-osteogenic FAK signaling appears to emanate primarily from the Y397 and Y925 phosphorylation sites and secondarily through the Y576/7 residue, but not from the Y861 residue, and these target ERK1/2, leading to increased osteogenic expression and matrix mineralization.

Acknowledgement: This work was supported by Public Health Service Grant 5R01EB002197 from the National Institute of Biomedical Imaging and Bioengineering (NIBIB) (to GEP) and by SEED funds from Rensselaer Polytechnic Institute.

Abbreviations

BSP-2	Bone sialoprotein-2 protein
COL-I	collagen-I
ERK	extracellular-related kinase
FAK	focal adhesion kinase
FTIR	Fourier transform infrared
GAPDH	glyceraldehyde-3-phosphate

	dehydrogenase
hMSC	human mesenchymal stem cells
MEK1	MAPK kinase
NEO	NEO blank vector infected hMSCs
NoV	Uninfected hMSCs
OP	Osteopontin protein
OSX	Osterix transcription factor
pERK	phosphorylated ERK
pFAK	phosphorylated FAK
qRT-PCR	quantitative real-time reverse transcriptase-polymerase chain reaction
RT-PCR	reverse transcriptase-polymerase chain reaction
WT	hMSCs infected with wild type FAK

References

1. Klees, R. F., Salasznyk, R. M., Boskey, A., & Plopper, G. E. (2006) *J. Cell Biochem.*

2. Loeser, R. F. (2002) *Biorheology* **39**, 119-124.

3. Salasznyk, R. M., Klees, R. F., Williams, W. A., Boskey, A., & Plopper, G. E. (2007) *Exp. Cell Res.* **313**, 22-37.

4. Suzawa, M., Tamura, Y., Fukumoto, S., Miyazono, K., Fujita, T., Kato, S., & Takeuchi, Y. (2002) *J. Bone Miner. Res.* **17**, 240-248.

5. Grigera, P. R., Jeffery, E. D., Martin, K. H., Shabanowitz, J., Hunt, D. F., & Parsons, J. T. (2005) *J. Cell Sci.* **118**, 4931-4935.

6. Hanks, S. K., Calalb, M. B., Harper, M. C., & Patel, S. K. (1992) *Proc. Natl. Acad. Sci. U. S. A* **89**, 8487-8491.

7. Mitra, S. K., Hanson, D. A., & Schlaepfer, D. D. (2005) *Nat. Rev. Mol. Cell Biol.* **6**, 56-68.

8. Parsons, J. T. (2003) *J. Cell Sci.* **116**, 1409-1416.

9. Zhao, J. H. & Guan, J. L. (2000) *Prog. Mol. Subcell. Biol.* **25:37-55.**, 37-55.

10. Cary, L. A., Chang, J. F., & Guan, J. L. (1996) *J. Cell Sci.* **109**, 1787-1794.

11. Toutant, M., Costa, A., Studler, J. M., Kadare, G., Carnaud, M., & Girault, J. A. (2002) *Mol. Cell Biol.* **22**, 7731-7743.

12. Hamilton, D. W. & Brunette, D. M. (2007) *Biomaterials* **28**, 1806-1819.

13. Salasznyk, R. M., Klees, R. F., Hughlock, M. K., & Plopper, G. E. (2004) *Cell Commun. Adhes.* **11**, 137-153.

14. Simmons, C. A., Matlis, S., Thornton, A. J., Chen, S., Wang, C. Y., & Mooney, D. J. (2003) *J. Biomech.* **36**, 1087-1096.

15. Xiao, G., Jiang, D., Thomas, P., Benson, M. D., Guan, K., Karsenty, G., & Franceschi, R. T. (2000) *J. Biol. Chem.* **275**, 4453-4459.

16. Katsumi, A., Milanini, J., Kiosses, W. B., del Pozo, M. A., Kaunas, R., Chien, S., Hahn, K. M., & Schwartz, M. A. (2002) *J. Cell Biol.* **158**, 153-164.

17. Laboureau, J., Dubertret, L., Lebreton-De, C. C., & Coulomb, B. (2004) *Exp. Dermatol.* **13**, 70-77.

18. Lin, T., Zeng, L., Liu, Y., DeFea, K., Schwartz, M. A., Chien, S., & Shyy, J. Y. (2003) *Circ. Res.* **92**, 1296-1304.

19. Tzima, E., del Pozo, M. A., Kiosses, W. B., Mohamed, S. A., Li, S., Chien, S., & Schwartz, M. A. (2002) *EMBO J.* **21**, 6791-6800.

20. Ward, D. F., Salasznyk, R. M., Klees, R. F., Backiel, J., Boskey, A., & Plopper, G. E. (2007) *Stem Cells Dev.* **16**, 467-480.

21. Boutahar, N., Guignandon, A., Vico, L., & Lafage-Proust, M. H. (2004) *J. Biol. Chem.* **279**, 30588-30599.

22. Tang, L., Lin, Z., & Li, Y. M. (2006) *Biochem. Biophys. Res. Commun.* **344**, 122-128.

23. Williams, W. A., Schapiro, N. E., Christy, S. R., Weber, G. L., Salasznyk, R. M., & Plopper, G. E. (2006) *Journal of Stem Cells* **1**, 173-182.

24. Boskey, A. L. (2006) *Curr. Osteoporos. Rep.* **4**, 71-75.

25. Ingber, D.E. (2006) *FASEB J.* **20**, 811-827.

26. Donaldson, C.L., Hulley, S.B., Vogel, J.M., Hattner, R.S., Bayers, J.H., and McMillan, D.E. (1970) *Metabolism* **19,** 1071-1084.

27. Rubin, C.T. and Lanyon, L.E. (1987) *J. Orthop. Res.* **5**, 300-310.

28. Nilsson, B.E. and Westlin, N.E. (1971) *Clin. Orthop. Relat Res.* **77,** 179-182.

29. Jones, H.H., Priest, J.D., Hayes, W.C., Tichenor, C.C., and Nagel, D.A. (1977) *J. Bone Joint Surg. Am.* **59**, 204-208.

30. Krolner, B., Toft, B., Pors, N.S., and Tondevold, E. (1983) *Clin. Sci. (Lond)* **64**, 541-546.

31. Judex, S. and Zernicke, R.F. (2000) *J. Appl. Physiol.* **88**, 2183-2191.

32. Liao, S. W., Hida, K., Park, J. S., & Li, S. (2004) *Conf. Proc. IEEE Eng Med. Biol. Soc.* **7**, 5024-5027.

33. Park, J. S., Chu, J. S., Cheng, C., Chen, F., Chen, D., & Li, S. (2004) *Biotechnol. Bioeng.* **88**, 359-368.

34. Campbell, J. J., Lee, D. A., & Bader, D. L. (2006) *Biorheology* **43**, 455-470.

35. Park, S. H., Sim, W. Y., Park, S. W., Yang, S. S., Choi, B. H., Park, S. R., Park, K., & Min, B. H. (2006) *Tissue Eng* **12**, 3107-3117.

36. Cho, T. J., Kim, J. A., Chung, C. Y., Yoo, W. J., Gerstenfeld, L. C., Einhorn, T. A., & Choi, I. H. (2007) *Calcif. Tissue Int.* **80**, 192-200.

37. Engler, A. J., Sen, S., Sweeney, H. L., & Discher, D. E. (2006) *Cell* **126**, 677-689.

38. Song, L. & Tuan, R. S. (2004) *FASEB J.* **18**, 980-982.

39. Earley, S. & Plopper, G. E. (2006) *Biochem. Biophys. Res. Commun.* **350**, 405-412.

40. Guignandon, A., Boutahar, N., Rattner, A., Vico, L., & Lafage-Proust, M. H. (2006) *Biochem. Biophys. Res. Commun.* **343**, 407-414.

41. Leucht, P., Kim, J. B., Currey, J. A., Brunski, J., & Helms, J. A. (2007) *PLoS. ONE.* **2**, e390.

42. Albinsson, S. & Hellstrand, P. (2007) *Am. J. Physiol Cell Physiol* **293**, C772-C782.

43. Glodek, A. M., Le, Y., Dykxhoorn, D. M., Park, S. Y., Mostoslavsky, G., Mulligan, R., Lieberman, J., Beggs, H. E., Honczarenko, M., & Silberstein, L. E. (2007) *Leukemia* **21**, 1723-1732.

44. Nagy, T., Wei, H., Shen, T. L., Peng, X., Liang, C. C., Gan, B., & Guan, J. L. (2007) *J. Biol. Chem.*

45. Kim, J. B., Leucht, P., Luppen, C. A., Park, Y. J., Beggs, H. E., Damsky, C. H., & Helms, J. A. (2007) *Bone* **41**, 39-51.

46. Takahashi, I., Onodera, K., Sasano, Y., Mizoguchi, I., Bae, J. W., Mitani, H., Kagayama, M., & Mitani, H. (2003) *Eur. J. Cell Biol.* **82**, 182-192.

47. Xiao, G., Gopalakrishnan, R., Jiang, D., Reith, E., Benson, M. D., & Franceschi, R. T. (2002) *J. Bone Miner. Res.* **17**, 101-110.

48. Chaudhary, L. R., Hofmeister, A. M., & Hruska, K. A. (2004) *Bone* **34**, 402-411.

49. Gersbach, C. A., Byers, B. A., Pavlath, G. K., & Garcia, A. J. (2004) *Exp. Cell Res.* **300**, 406-417.

50. Luppen, C. A., Smith, E., Spevak, L., Boskey, A. L., & Frenkel, B. (2003) *J. Bone Miner. Res.* **18**, 1186-1197.